ADVANCED
MATERIALS

Supporting Information

for *Adv. Mater.*, DOI: 10.1002/adma.201604260

Confined Metastable 2-Line Ferrihydrite for Affordable Point-of-Use Arsenic-Free Drinking Water

*Avula Anil Kumar, Anirban Som, Paolo Longo, Chennu Sudhakar, Radha Gobinda Bhuin, Soujit Sen Gupta, Anshup, Mohan Udhaya Sankar, Amrita Chaudhary, Ramesh Kumar, and Thalappil Pradeep**

Supporting Information

for *Adv. Mater.*, DOI: 10.1002/adma.201604260

Confined metastable 2-line ferrihydrite for affordable point-of-use arsenic free drinking water

*Avula Anil Kumar[1], Anirban Som[1], Paolo Longo[2], Chennu Sudhakar[1], Radha Gobinda Bhuin[1], Soujit Sen Gupta[1], Anshup[1], Mohan Udhaya Sankar[1], Amrita Chaudhary[1], Ramesh Kumar[1] and Thalappil Pradeep[1]**

Supporting Information Text

Materials and Methods

High Resolution Transmission Electron Microscopy (HRTEM) images of the sample were obtained with JEM 3010 (JEOL, Japan) operating at 200 kV with an ultra-high resolution (UHR) pole piece. Elemental mapping on TEM was done on an Oxford semi STEM EDS system. The samples for HRTEM were prepared by dropping the dispersion on amorphous carbon films supported on a copper grid and dried. Surface morphology, elemental analysis and elemental mapping studies were carried out using a Scanning Electron Microscope (SEM) equipped with Energy Dispersive Analysis of X-rays (EDAX) (FEI Quanta 200). For the SEM and EDAX measurements, samples were spotted on the aluminium sample stub. Annular Dark-Field Scanning Tunneling Electron Microscopy (ADF STEM) measurements were carried out using a Gatan GIF Quantum ER fully loaded Tecnai F20. This analysis was carried out at 200 kV and data acquired in digital micrograph and chemical analysis was carried out with 1 eV energy resolution. This entire ADF STEM analysis was carried out in DualEELS (Dual Electron Energy Loss Spectroscopy) mode to measure the accurate chemical shift. X-ray Photoelectron Spectroscopy (XPS) measurements were done using ESCA Probe TPD spectrometer of Omicron Nanotechnology. Polychromatic Mg Kα was used as the X-ray source (hν = 1253.6 eV). The samples were spotted as drop-cast films on a sample stub. Constant analyzer energy of 20 eV was used for the measurements. Binding energy was calibrated with respect to C 1s at 284.5 eV. Total arsenic and iron concentrations in water were detected using inductively coupled plasma mass spectrometry (ICP-MS) (Agilent Technologies, 7700x ICP-MS and PerkinElmer NexION 300D ICP-MS) with appropriate standards.

Mechanical testing of CM2LF: The shear strength of the composite was measured at dry and wet conditions, separately. Around ~ 90 g of granular media was packed in a 6 cm x 6 cm x 6 cm (L x B x H) sample holder and horizontal shear stress was measured under normal stress of 50, 100 and 200 kPa, respectively.

Supporting Information Figures

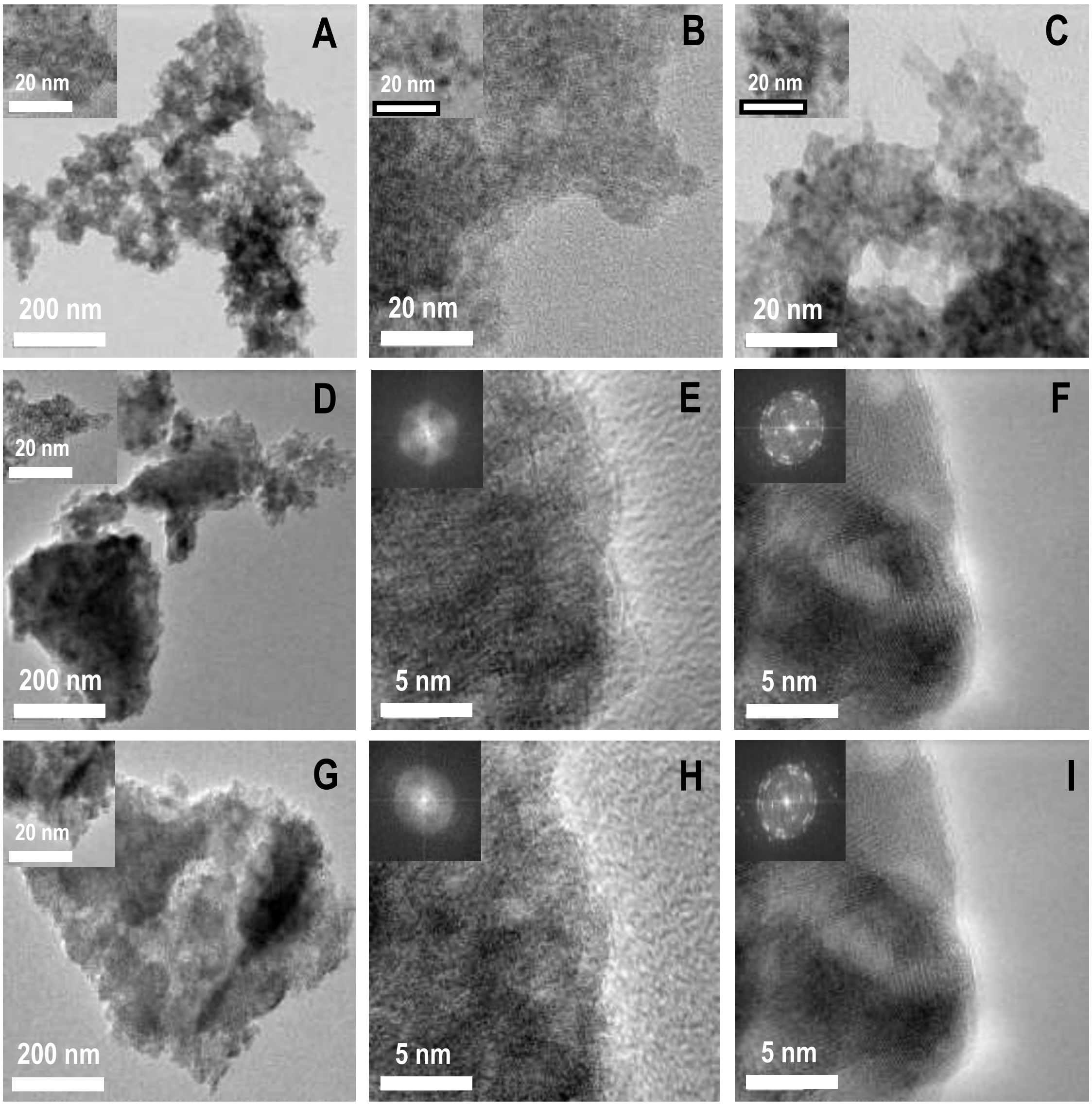

Figure S1. Time dependent TEM images of CM2LF, (A, D and G) initial material, As(III) adsorbed and As(V) adsorbed CM2LF before electron beam irradiation showing amorphous nature of the material (the insets shows the high resolution images). (B, E and H) Short time electron beam induced crystallization of the initial, As(III) adsorbed and As(V) adsorbed CM2LF showing a little crystalline behavior of the material (inset images). (C, F and I) Long time electron beam induced crystallization of the initial, As(III) adsorbed and As(V) adsorbed CM2LF showing the more crystalline nature of the material (inset images).

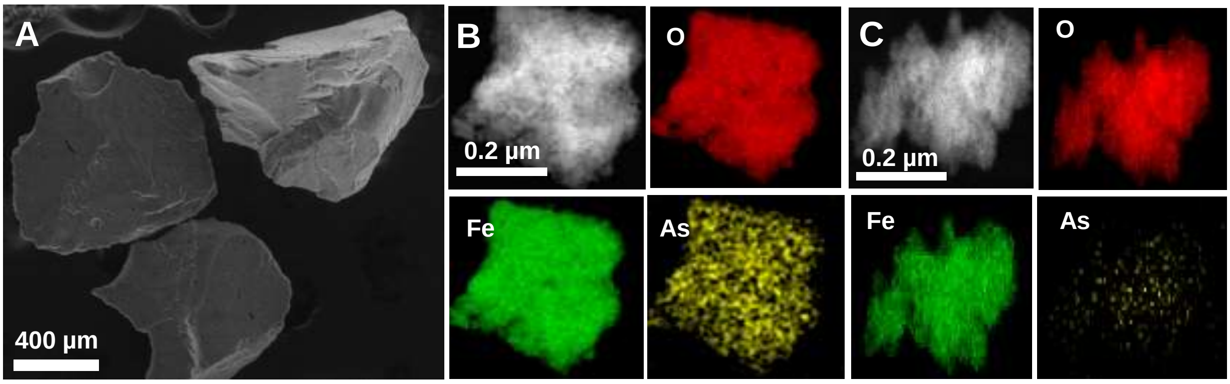

Figure S2. (A) SEM image of the initial granular material (52 X 72 µm), which was stored in water for about 6 months. (B and C) ADF-STEM images of As(III) and As(V) adsorbed material, respectively and the corresponding elemental maps of O, Fe and As(III).

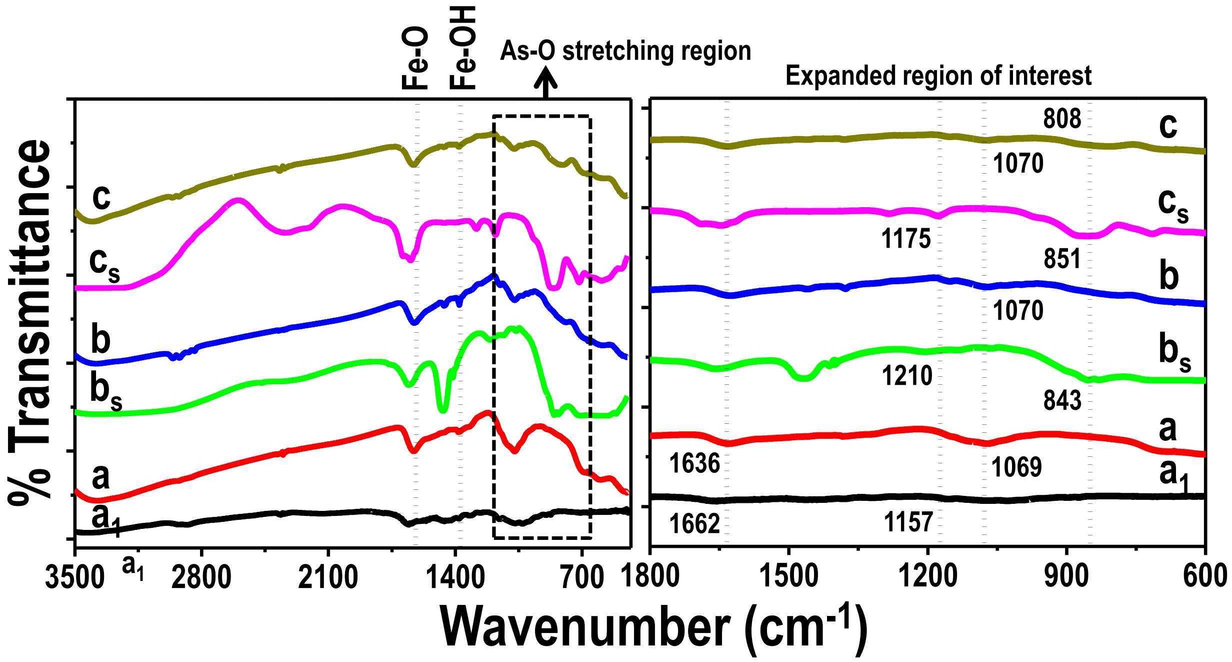

Figure S3. Infrared spectrum (IR) of (a_1) bio-polymer (chitosan), (a) the initial material (i.e., CM2LF), (b) after As(III) adsorption and (c) after As(V) adsorption on CM2LF, independently compared with respective arsenic standards (b_s) As(III) standard and (c_s) As(V) standard, respectively and the corresponding stretching and bending region of Fe-O, Fe-OH and As-O are shown in the expanded region. The corresponding peak shifting are also shown in the expanded region.

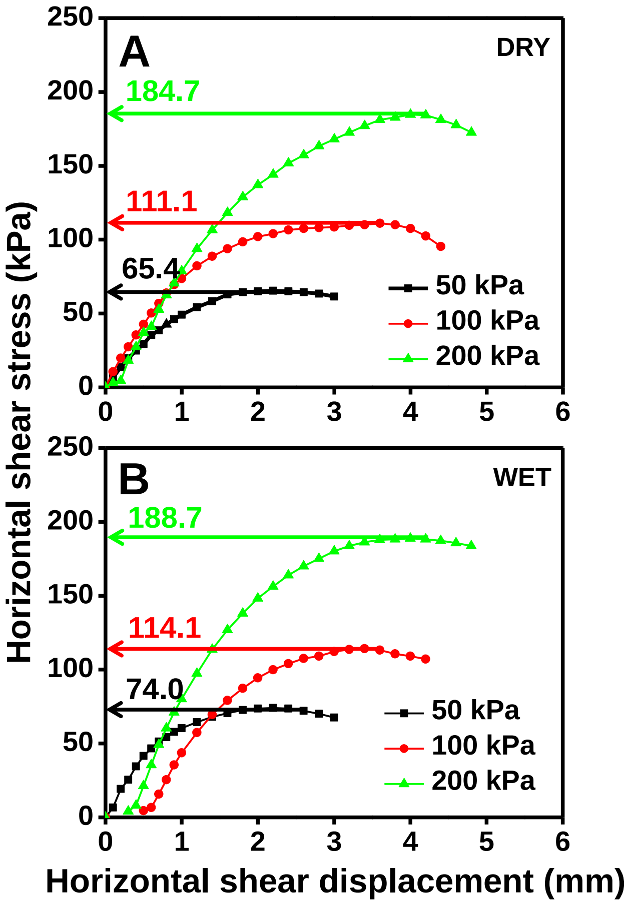

Figure S4. Direct shear test of CM2LF. (A and B) Plot of horizontal shear stress vs. horizontal shear displacement of loosely packed CM2LF measured at dry condition (A) and wet condition (B), respectively.

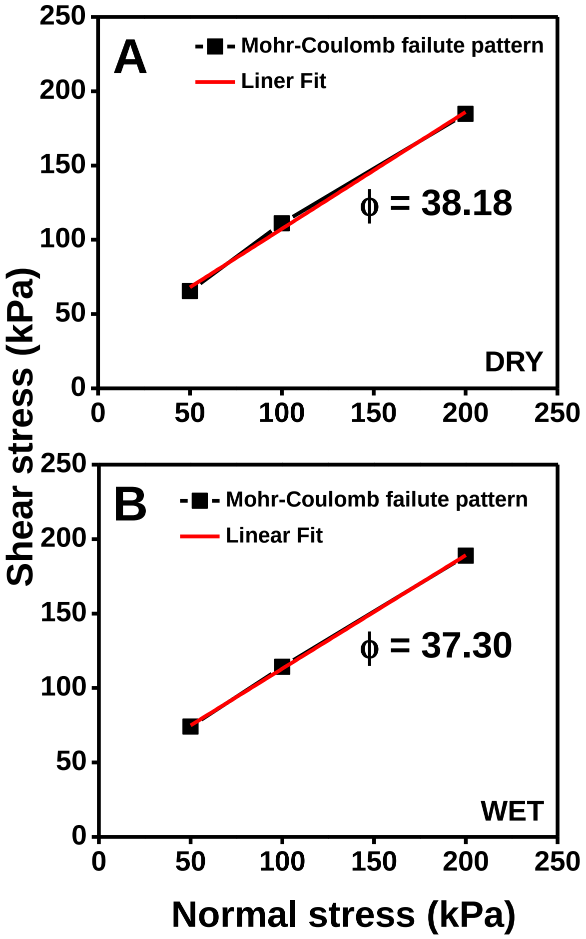

Figure S5. Mohr-Coulomb failure pattern of CM2LF. (A and B) Plot of shear stress vs. normal stress of loosely packed CM2LF showing the straight-line approximation of the Mohr-Coulomb failure pattern measured at dry condition (A) and wet condition (B), respectively.

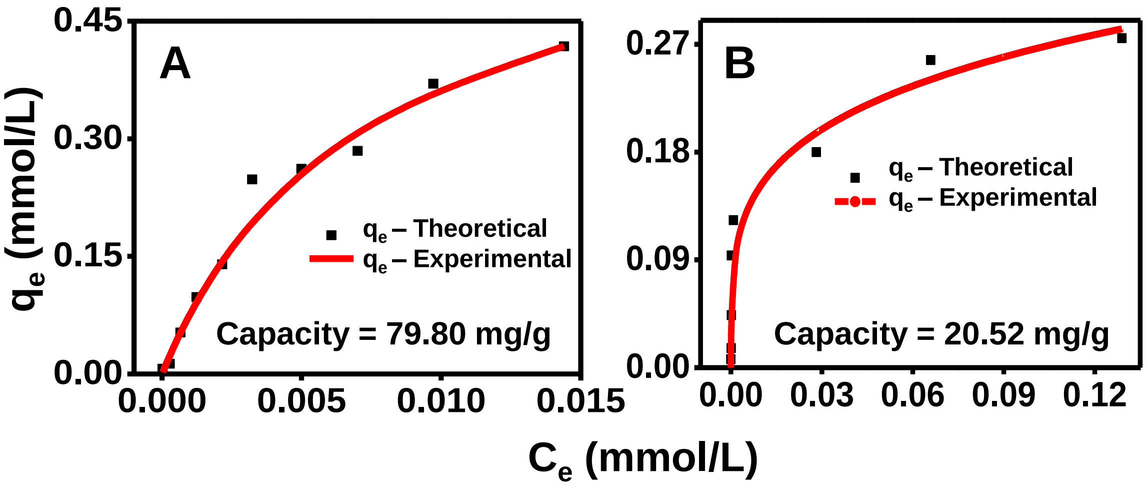

Figure S6. Arsenic uptake kinetics of CM2LF for As(III) and As(V). (A and B) Langmuir isotherm for As(III) adsorbed (mmol/g) as a function of As(III) concentration (mmol/L) (A) and Langmuir isotherm for As(V) adsorbed (mmol/g) as a function of As(V) concentration (mmol/L) (B) conducted with 30 mg initial adsorbent dose in 30 mL deionized water with 90 min as contact time, respectively. Fitted curve is based on Langmuir isotherm.

Arsenic adsorption isotherm of as-synthesized CM2LF composite was measured in the lab in 0.04 M NaCl at pH 7.0, to mimic field conditions. As-synthesized composite adsorbs approximately 1.064 mmol/g and 0.27 mmol/g each at an equilibrium concentration of 0.15 mM of As(III) and As(V), respectively. Langmuir isotherm was evaluated using Equation (1).

$$\frac{C_e}{q_e} = \frac{C_e}{q_{max}} + \frac{1}{q_{max}b}$$ Equation (1)

where, C_e (mmol/L) is the equilibrium concentration of arsenic in the solution, q_e (mmol/L) is the quantity of arsenic adsorbed at equilibrium and q_{max} (mmol/L) is the monolayer adsorption capacity, and b (L/mmol) is the Langmuir adsorption constant, related to the free energy of adsorption.

The Langmuir isotherm was used to estimate the maximum adsorption capacity of CM2LF under the conditions 298 K, pH 7.0 with 90 min of contact time and 1.0 g/L adsorbent dose while varying initial arsenic concentration from 0.5 to 30 mg/L. The values of the isotherm constants $1/q_{max}$ and $1/q_{max}b$, for As(III) adsorption are 1.60 and 0.0114, respectively while that for As(V) adsorption are 3.63 and 0.008, respectively.

The linear plot of C_e/q_e versus C_e (mmol/L) along with a high value correlation coefficient indicates that Langmuir isotherm provides a better fit of the equilibrium data. The Langmuir monolayer capacity (mg/g) of CM2LF for As(III) adsorption is calculated to be 79.80 mg/g while for As(V) adsorption is 20.52 mg/g. This difference is because the adsorbent works better at higher concentrations of As(III) and at lower concentrations of As(V). This is because basic pH is more suitable to remove As(III) while acidic pH is more suitable to remove As(V). The Langmuir model is based on the assumption of homogeneous monolayer coverage with all adsorption sites being identical and energetically equivalent.

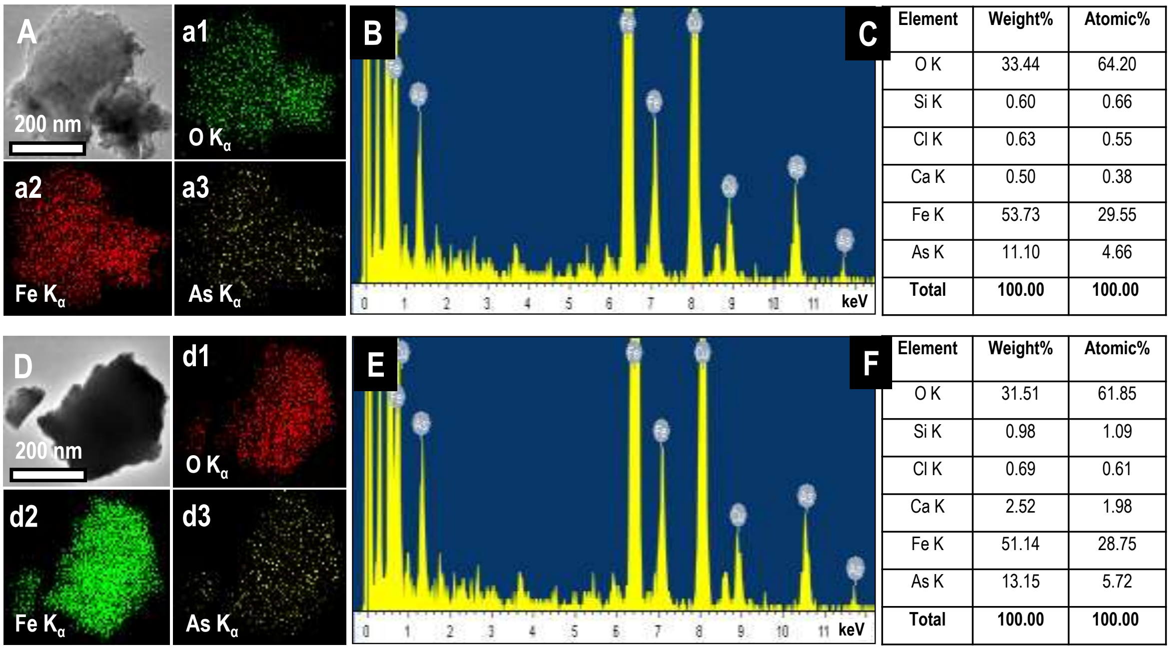

Element	Weight%	Atomic%
O K	33.44	64.20
Si K	0.60	0.66
Cl K	0.63	0.55
Ca K	0.50	0.38
Fe K	53.73	29.55
As K	11.10	4.66
Total	**100.00**	**100.00**

Element	Weight%	Atomic%
O K	31.51	61.85
Si K	0.98	1.09
Cl K	0.69	0.61
Ca K	2.52	1.98
Fe K	51.14	28.75
As K	13.15	5.72
Total	**100.00**	**100.00**

Figure S7. TEM-EDX analysis of CM2LF. (A) X-ray elemental mapping of different elements, (B) Elemental EDX spectrum and (C) Elemental EDX analysis of As(III) adsorbed CM2LF. Same data for As(V) adsorbed CM2LF.

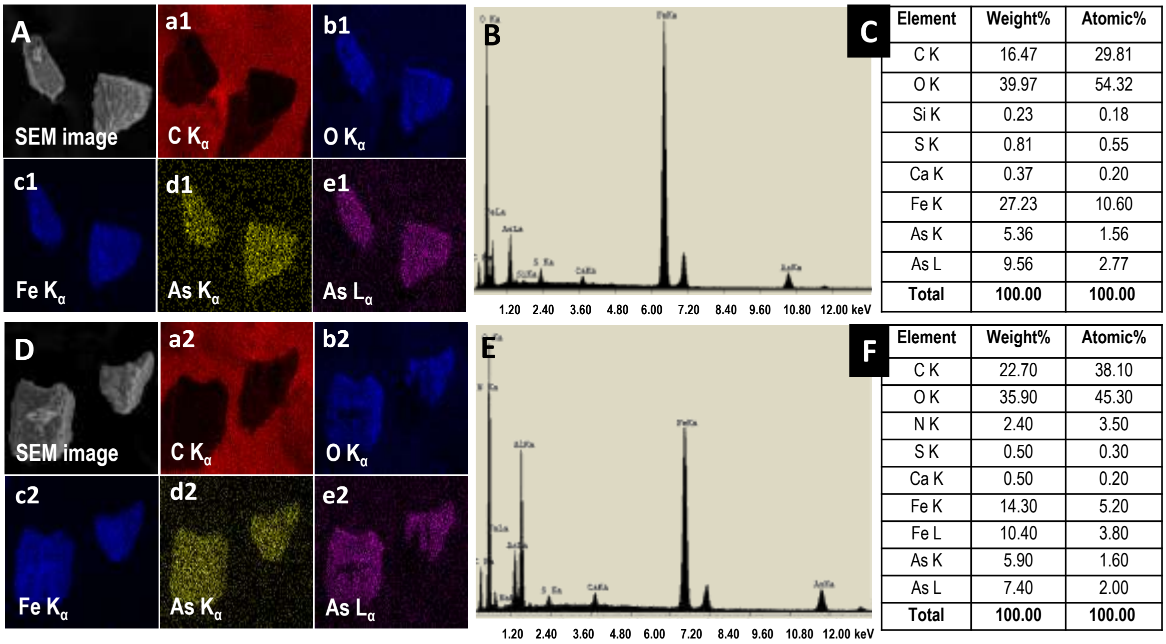

C

Element	Weight%	Atomic%
C K	16.47	29.81
O K	39.97	54.32
Si K	0.23	0.18
S K	0.81	0.55
Ca K	0.37	0.20
Fe K	27.23	10.60
As K	5.36	1.56
As L	9.56	2.77
Total	**100.00**	**100.00**

F

Element	Weight%	Atomic%
C K	22.70	38.10
O K	35.90	45.30
N K	2.40	3.50
S K	0.50	0.30
Ca K	0.50	0.20
Fe K	14.30	5.20
Fe L	10.40	3.80
As K	5.90	1.60
As L	7.40	2.00
Total	**100.00**	**100.00**

Figure S8. SEM-EDX analyses of CM2LF: (A) X-ray elemental mapping of different elements, (B) Elemental EDX spectrum and (C) Elemental EDX analysis of As(III) adsorbed CM2LF, respectively. Same data for As(V) adsorbed CM2LF.

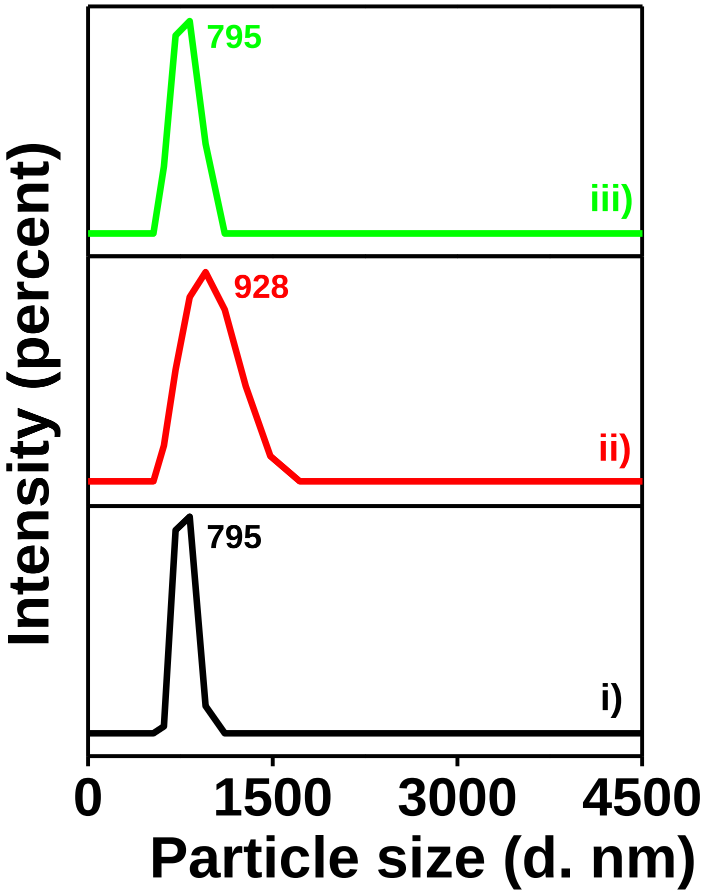

Figure S9. Dynamic light scattering (DLS) analysis of arsenic in presence of iron (Fe-As interaction) in solution. The Fe(II)/Fe(III) hydroxide particulates in presence of (i) As(III), (ii) As(V) and (iii) As(Mix.), which is showing the existence of only single major particle size distributions (~ 0.8 µm – 1 µm) in water.

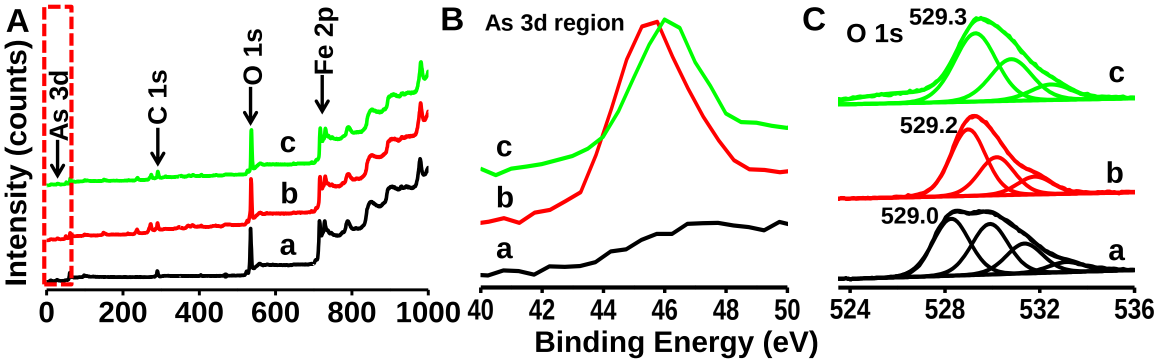

Figure S10. (A) X-ray photoelectron spectrum (XPS) analysis of CM2LF and (B) is the As 3d expanded region of the same plot (a) before As adsorption (b) after As(III) adsorption and (c) after As(V) adsorption. (C) Deconvoluted XPS spectrum of O 1s of CM2LF (a) before As adsorption (b) after As(III) adsorption and (c) after As(V) adsorption.

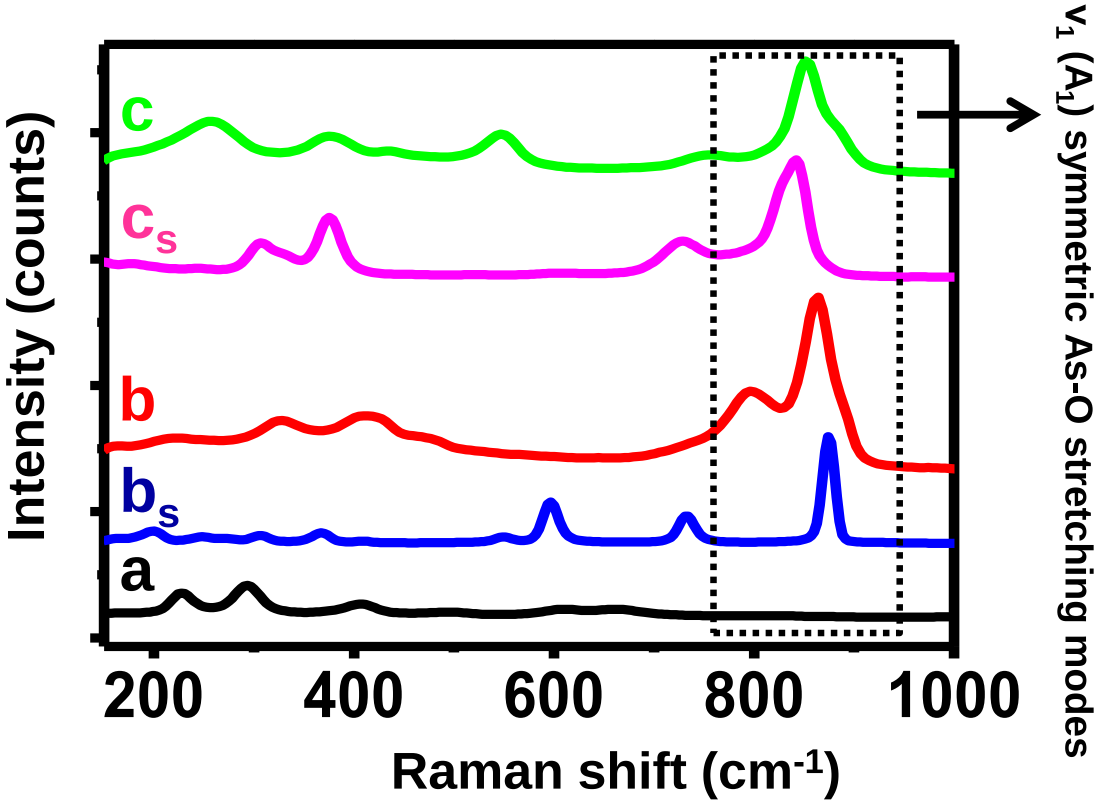

Figure S11. Raman spectrum of (A) CM2LF, (b_s) standard As(III) in solid state, (b) As(III) after treated with CM2LF, (c_s) standard As(V) in solid state and (c) A(V) after treated with CM2LF.

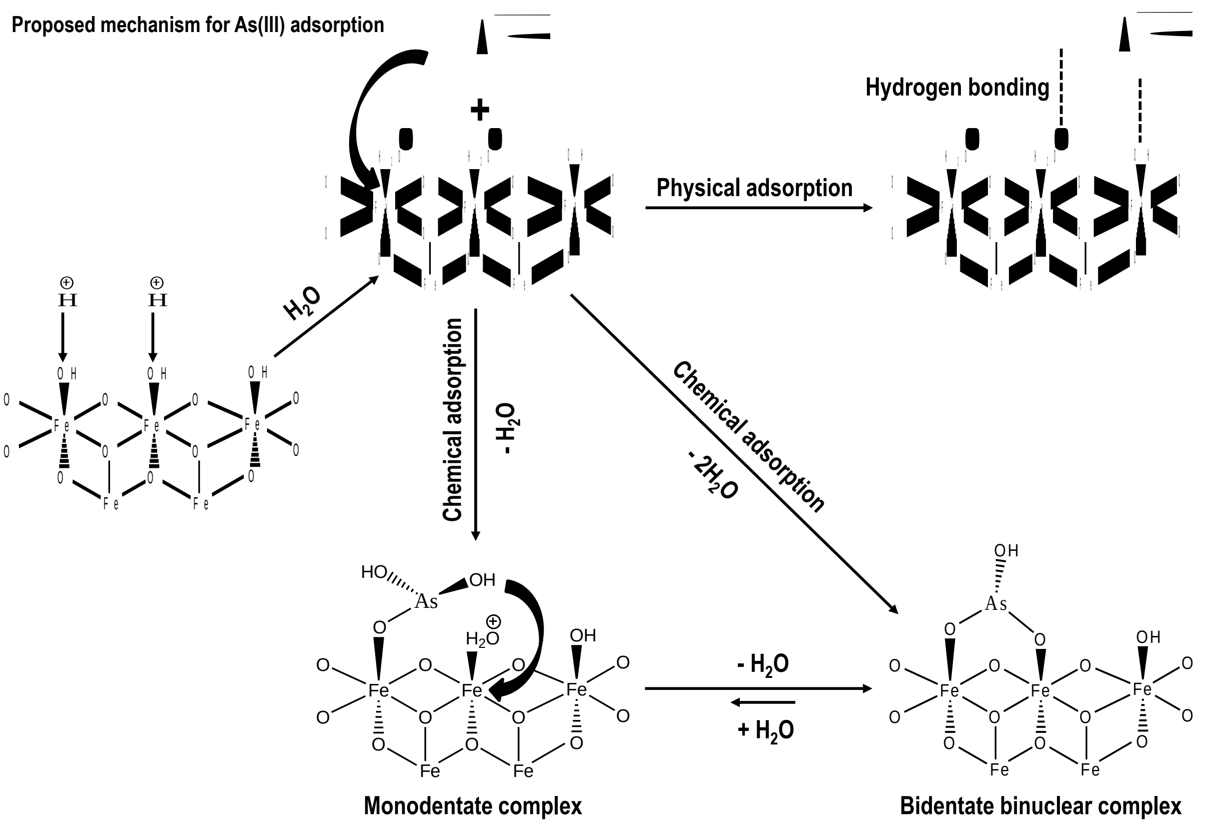

Figure S12. Adsorption mechanism of As(III) on CM2LF.

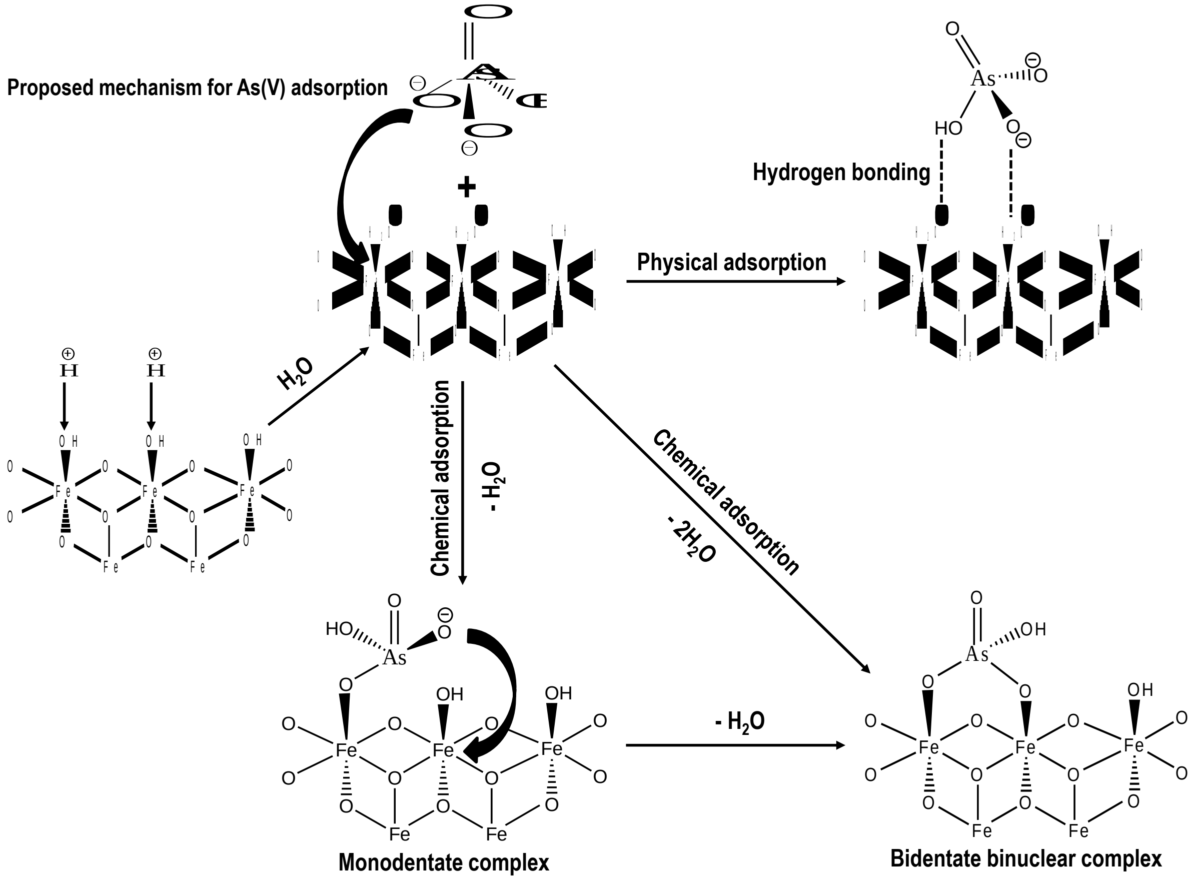

Figure S13. Adsorption mechanism of As(V) on CM2LF.

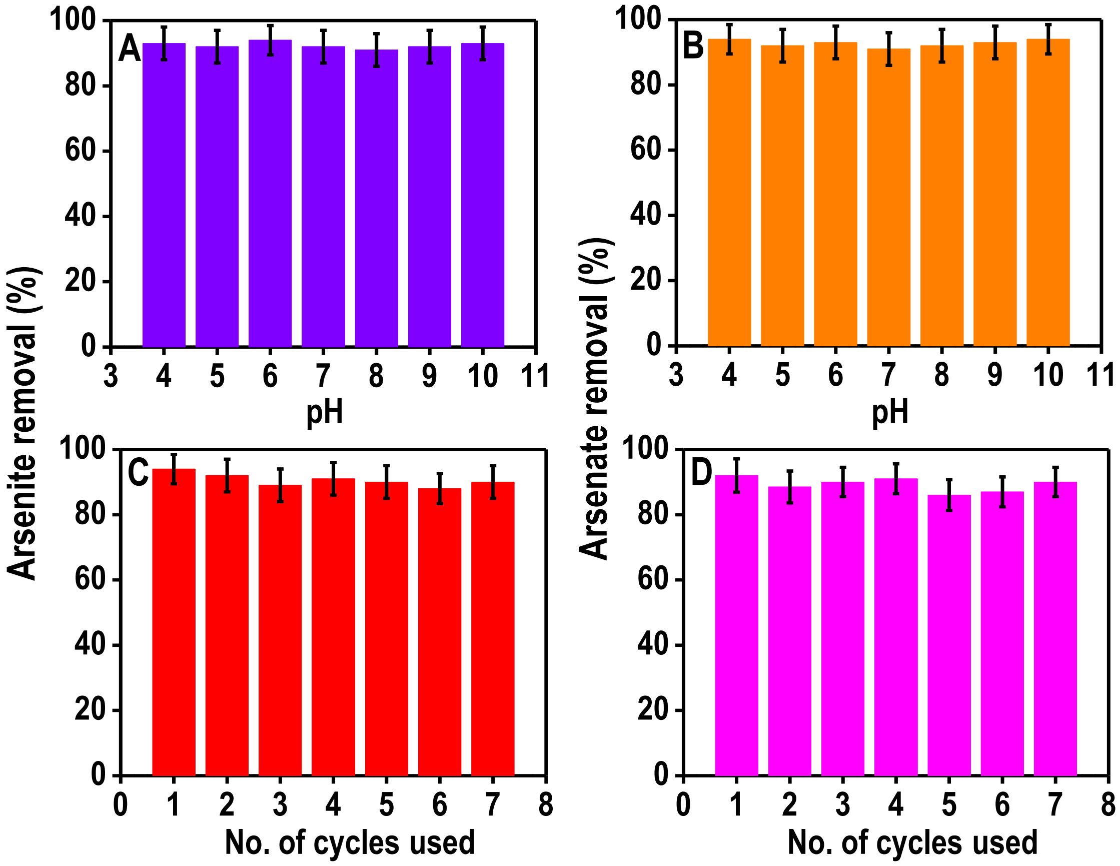

Figure S14. Adsorption efficiency of CM2LF for (A) As(III) and (B) As(V) as a function of pH. The re-use performance of the CM2LF composite upon activation for (C) As(III) and (D) As(V) removal (batch study) as a function of no. of cylces. An input arsenic concentration of 1.1 mg L^{-1} was used for both the species. Volume taken as 100 mL of ground water for 25 mg of the composite and the incubation time was 90 min.

.

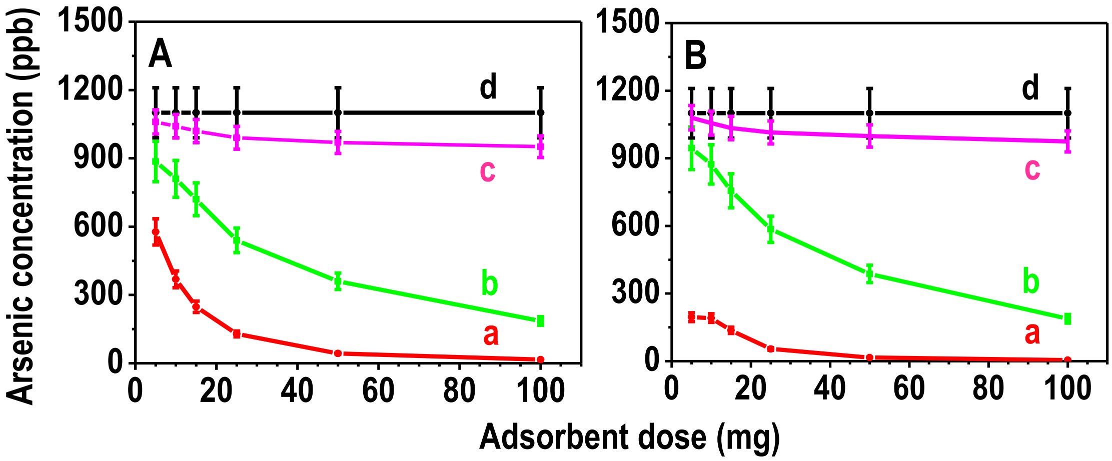

Figure S15. Performance data (batch study) of arsenic removal capacity of CM2LF compared with pure ferrihydrite and chiotsan. Residual (A) arsenite and (B) arsenate concentrations as a function of (a) CM2LF dosage, in comparison to (b) pure ferrihydrite and (c) chitosan, with an input arsenic concentration of 1.1 mg L^{-1}, which is shown as (d). Volume taken was 100 mL of ground water, for different doses, varying from 5-100 mg of the materials and the incubation time was 90 min.

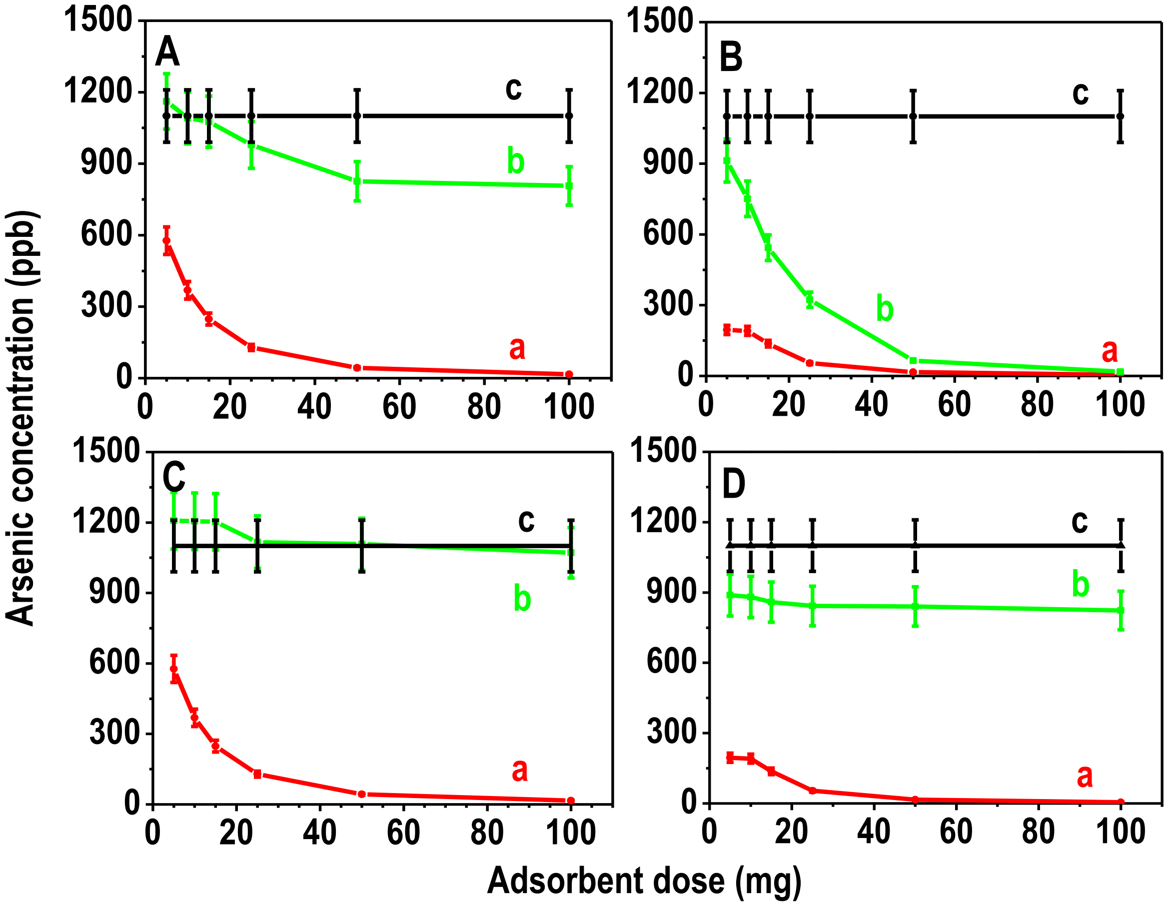

Figure S16. Performance data (batch study) of arsenic removal capacity of CM2LF compared with activated alumina and activated carbon. (A and B) Residual arsenite (A) and arsenate (B) concentrations as a function of (a) CM2LF dosage in comparison to (b) activated alumina with an (c) input arsenic concentration of 1.1 mg L^{-1}. (C and D) Residual arsenite (C) and arsenate (D) concentrations as a function of (a) CM2LF dosage in comparison to (b) activated carbon with an (c) input arsenic concentration of 1.1 mg L^{-1}. Volume taken was 100 mL ground water and the incubation time was 90 min.

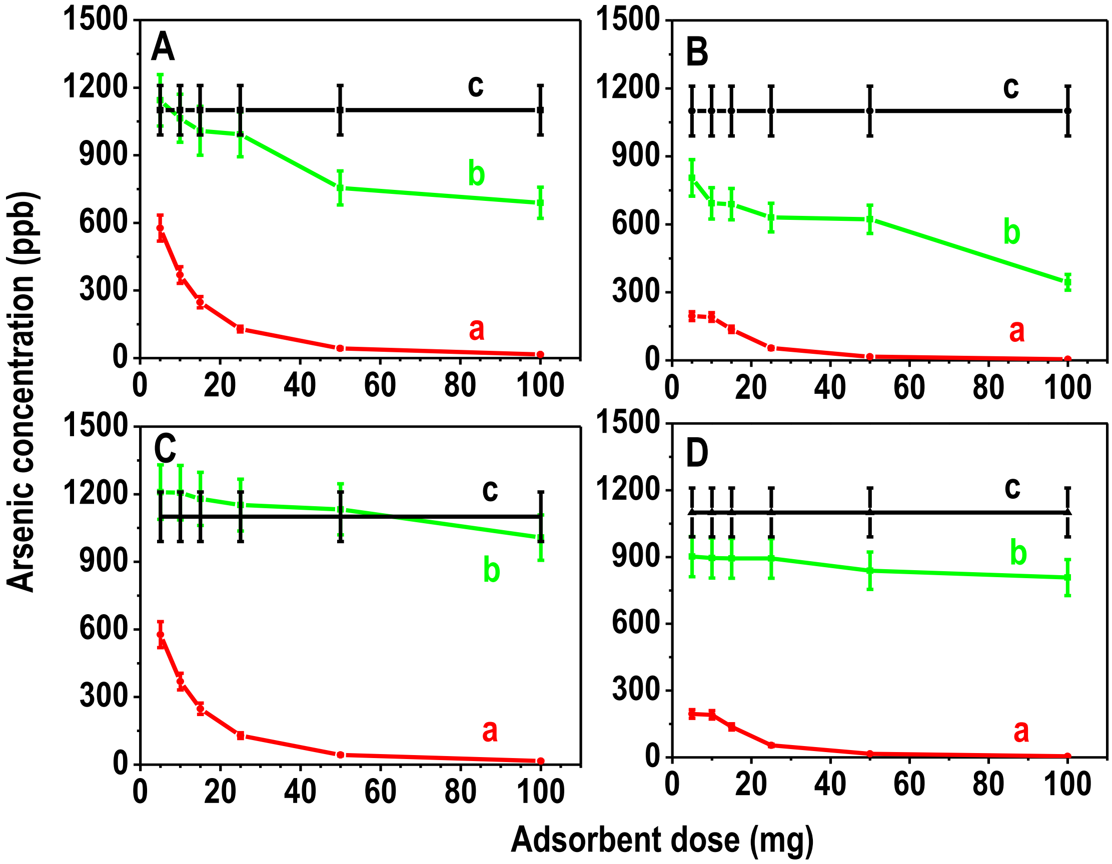

Figure S17. Performance data (batch study) of CM2LF in comparison to iron oxide (Fe_2O_3) and silicon dioxide (SiO_2) with respect to arsenic removal. (A and B) Residual arsenite (A) and arsenate (B) concentrations as a function of (a) CM2LF dosage in comparison to (b) iron oxide dosage with an (c) input arsenic concentration of 1.1 mg L^{-1}. (C and D) Residual arsenite (C) and arsenate (D) concentrations as a function of (a) CM2LF dosage in comparison to (b) silicon dioxide dosage with an (c) input arsenic concentration of 1.1 mg L^{-1}. Volume taken was 100 mL ground water and incubation time was 90 min.

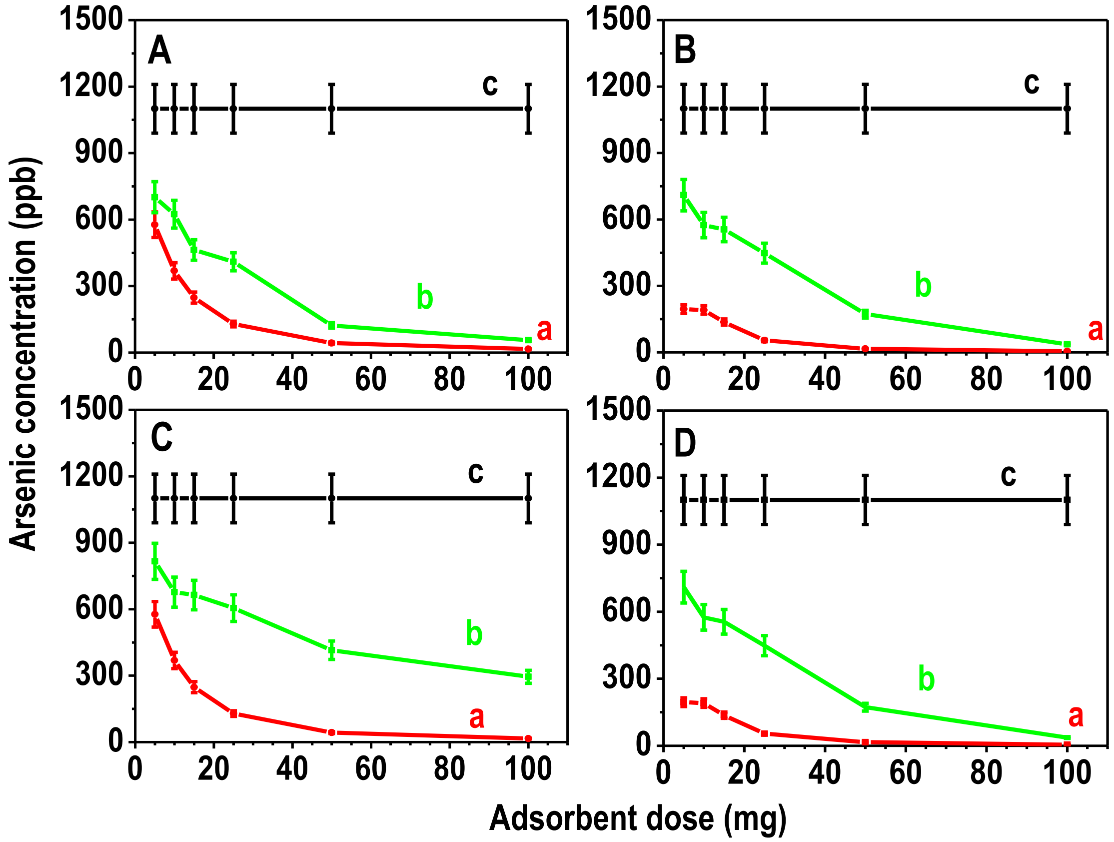

Figure S18. Performance data (batch study) of CM2LF in comparison to granular ferric hydroxide (GFH) and organic templated boehmite nanostructure (OTBN) with respect to arsenic removal. (A and B) Residual arsenite (A) and arsenate (B) concentrations as a function of (a) CM2LF dosage in comparison to (b) GFH dosage with an (c) input arsenic concentration of 1.1 mg L^{-1}. (C and D) Residual arsenite (C) and arsenate (D) concentrations as a function of (a) CM2LF dosage in comparison to (b) OTBN dosage, respectively with an (c) input arsenic concentration of 1.1 mg L^{-1}. Volume taken was 100 mL ground water and incubation time was 90 min.

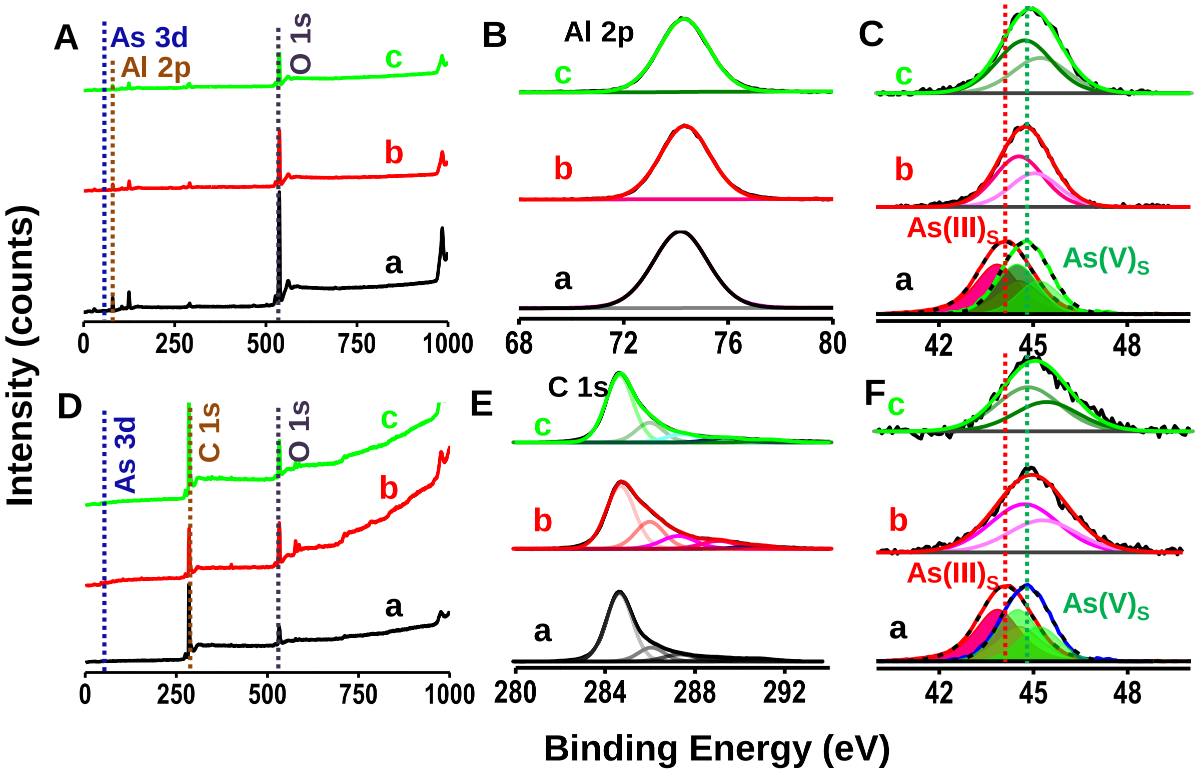

Figure S19. XPS data of activated alumina and activated carbon upon arsenic adsorption. (A) Survey spectrum, (B) Aluminium 2p (Al 2p) region and (C) Arsenic 3d (As 3d) region of activated alumina (a) before As adsorption, (b) after As(III) adsorption and (c) after As(V) adsorption, independently compared with (b_s) standard As(III) and (c_s) standard As(V), respectively. (D) Survey spectrum, (E) Carbon 1s (C 1s) region and (F) Arsenic 3d (As 3d) region of activated carbon (a) before As adsorption, (b) after As(III) adsorption and (c) after As(V) adsorption, independently compared with (b_s) standard As(III) and (c_s) standard As(V), respectively.

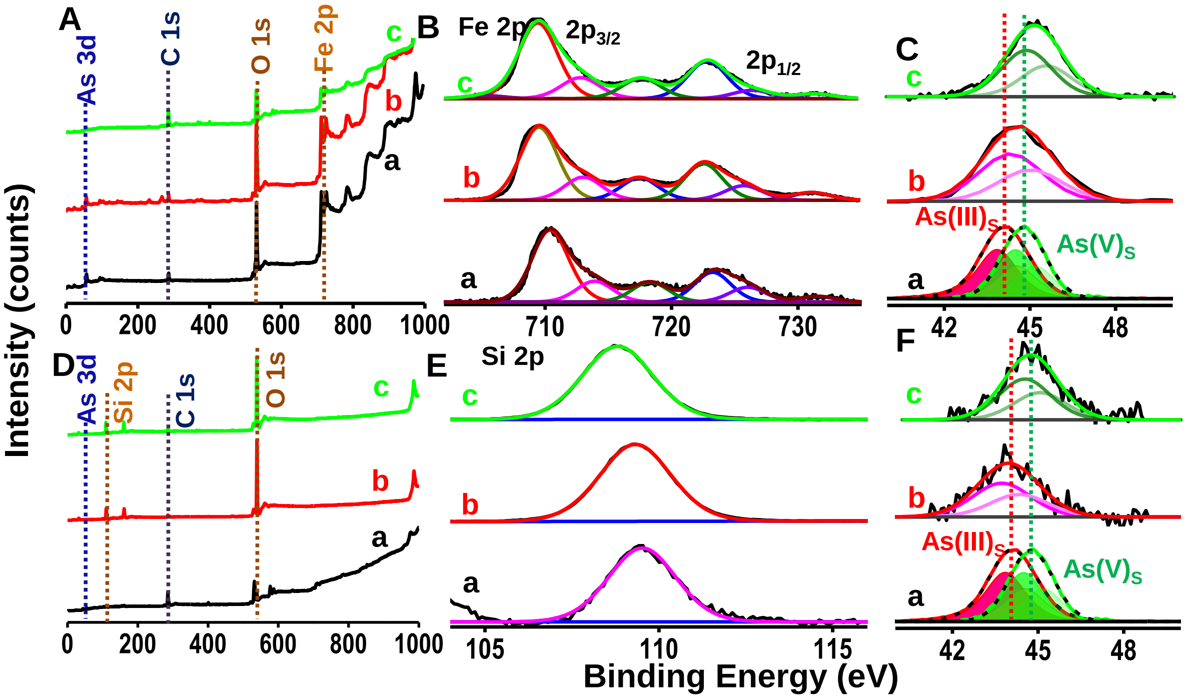

Figure S20. XPS data of iron oxide and silicon dioxide upon arsenic adsorption. (A) Survey spectrum, (B) Iron 2p (Fe 2p) region and (C) Arsenic 3d (As 3d) region of iron oxide (a) before As adsorption, (b) after As(III) adsorption and (c) after As(V) adsorption, independently compared with (b_s) standard As(III) and (c_s) standard As(V), respectively. (D) Survey spectrum, (E) Silicon 2p (Si 2p) region and (F) Arsenic 3d (As 3d) region of silicon dioxide (a) before As adsorption, (b) after As(III) adsorption and (c) after As(V) adsorption, independently compared with (b_s) standard As(III) and (c_s) standard As(V), respectively.

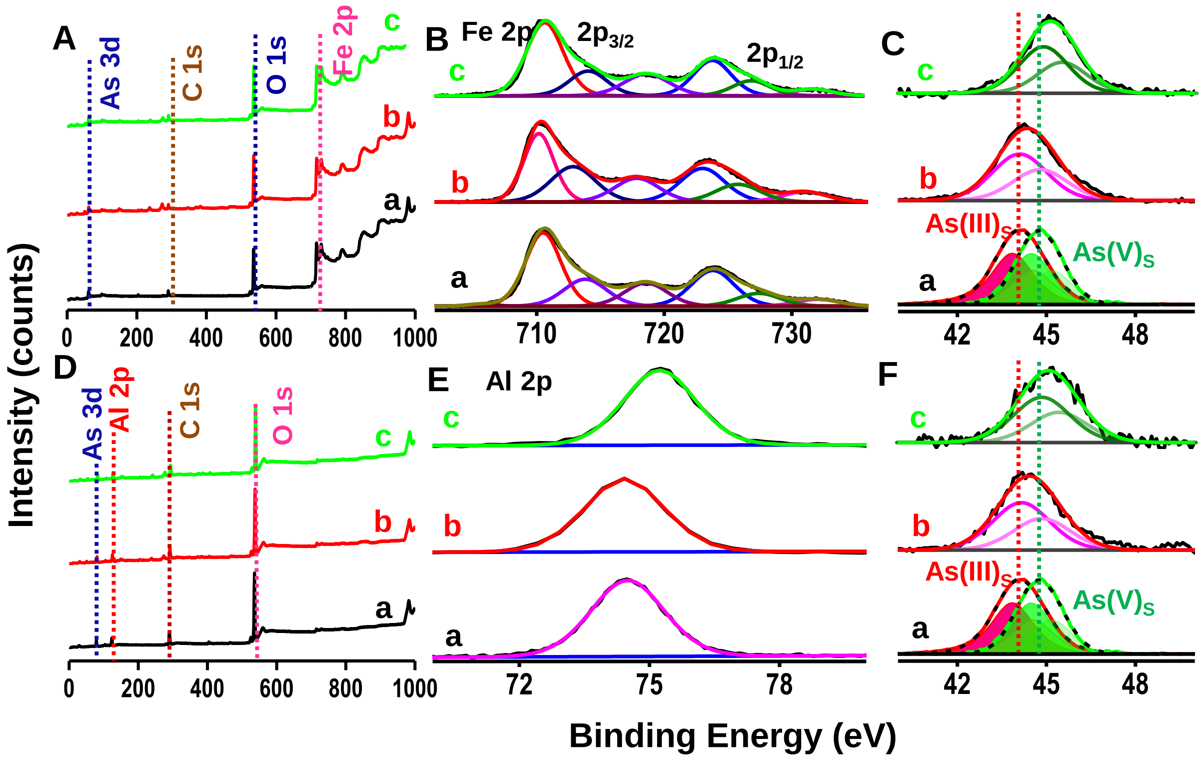

Figure S21. XPS data of GFH and OTBN upon arsenic adsorption. (A) Survey spectrum, (B) Iron 2p (Fe 2p) region and (C) Arsenic 3d (As 3d) region of GFH (a) before As adsorption, (b) after As(III) adsorption and (c) after As(V) adsorption, independently compared with (b_s) standard As(III) and (c_s) standard As(V), respectively. (D) Survey spectrum, (E) Aluminium 2p (Al 2p) region and (F) Arsenic 3d (As 3d) region of OTBN (a) before As adsorption, (b) after As(III) adsorption and (c) after As(V) adsorption, independently compared with (b_s) standard As(III) and (c_s) standard As(V), respectively.

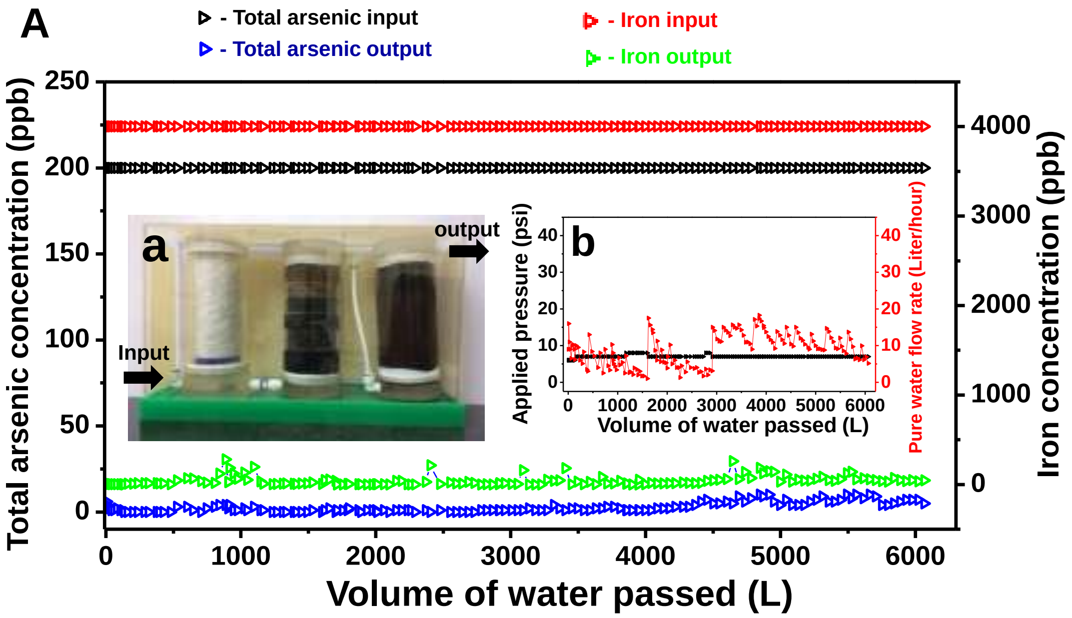

Figure S22. (A) Performance data for the removal of arsenic and iron. Inset (a) shows the proof of concept prototype of Inline domestic unit for removal of arsenic (As(III) + As(V)) and iron (Fe(II) + Fe (III)) contamination from water using three stage filtration, having first cartridge with 0.5 µm polypropylene yarn-wound candle filter for removal of micro-particulates, second cartridge with iron removal media and third cartridge with 900 g arsenic adsorbent. Inset (b) shows pure water flow rate from the unit at corresponding applied pressure. Slight variation in flow rate is due to the change in head pressure in week long experiments.

Table S1.

Arsenic uptake capacity of CM2LF under various ionic strengths with an input arsenic concentration of 1.1 mg L^{-1}, respectively for both As(III) and As(V). 100 mL arsenic contaminated ground water was taken for 25 mg of the composite and the incubation time was 90 min.

Type of ion	Concentration of ion used	Input As(III)	Uptake As(III)	Input As(V)	Uptake As(V)
Fluoride	0.6 ppm	1.1 ppm	1.09 ppm	1.1 ppm	1.09 ppm
Chloride	87 ppm	1.1 ppm	1.09 ppm	1.1 ppm	1.08 ppm
Nitrate	1.9 ppm	1.1 ppm	1.09 ppm	1.1 ppm	1.10 ppm
Sulphate	33 ppm	1.1 ppm	1.09 ppm	1.1 ppm	1.09 ppm
Silicate	16 ppm	1.1 ppm	1.09 ppm	1.1 ppm	1.09 ppm
Sodium	54 ppm	1.1 ppm	1.08 ppm	1.1 ppm	1.10 ppm
Potassium	2.5 ppm	1.1 ppm	1.09 ppm	1.1 ppm	1.10 ppm
Magnesium	15 ppm	1.1 ppm	1.09 ppm	1.1 ppm	1.09 ppm
Calcium	29 ppm	1.1 ppm	1.09 ppm	1.1 ppm	1.09 ppm
Carbonate	100 ppm	1.1 ppm	1.09 ppm	1.1 ppm	1.09 ppm
Bicarbonate	100 ppm	1.1 ppm	1.09 ppm	1.1 ppm	1.09 ppm

Table S2.

ToC leaching from various components used in making the CM2LF composite in comparison to the CM2LF before and after arsenic saturation. Volume taken was 100 mL Milli-Q water for 100 mg of the composite and the incubation time was 90 min. Milli-Q water was taken for the experiments for the composite, as the tap water routinely shows a ToC of 8.60 ppm.

Sample analysed	**ToC**
Blank water	0.17 ppm
Blank Chitosan	3.39 ppm
Chitosan @ pH 9	0.57 ppm
CM2LF without Arsenic	0.65 ppm
Saturated CM2LF with As(III)	0.69 ppm
Saturated CM2LF with As(V)	0.76 ppm

Table S3.

Physicochemical characteristics of influent natural water.

(Note: All parameters are expressed in mg L^{-1}, except for pH and conductivity)

Parameters	**Value**
Total coliforms (CFU/mL)	1-2 x 10^3
pH @ 25°C	7.8
Conductivity (µS/cm)	640.0
Fluoride	0.57
Chloride	86.34
Nitrate	1.84
Sulphate	32.41
Silicate	15.87
Lithium	ND
Sodium	53.74
Ammonium	ND
Potassium	2.33
Magnesium	14.34
Calcium	28.72

ND - not detected

Natural drinking water (without treatment so that there is a residual bacterial count in it) was used for testing to ensure that the material functions in the field.